Korean J. Chem. Eng., 33(4), 1425-1430 (2016)
DOI: 10.1007/s11814-015-0268-7

pISSN: 0256-1115
eISSN: 1975-7220

Accurate measurement of phase equilibria and dissociation enthalpies of HFC-134a hydrates in the presence of NaCl for potential application in desalination

Dongyoung Lee*,‡, Yohan Lee*,‡, Wonjung Choi*, Seungmin Lee, and Yongwon Seo*,†**

*School of Urban and Environmental Engineering, Ulsan National Institute of Science and Technology, Ulsan 44919, Korea
**Offshore Plant Resources R&D Center, Korea Institute of Industrial Technology, Busan 46749, Korea
(*Received 29 October 2015 • accepted 2 December 2015*)

Abstract−Phase equilibria, structure identification, and dissociation enthalpies of HFC-134a hydrates in the presence of NaCl are investigated for potential application in desalination. To verify the influence of NaCl on the thermodynamic hydrate stability of the HFC-134a hydrate, the three-phase (hydrate (H) - liquid water (L_W) - vapor (V)) equilibria of the HFC-134a+NaCl (0, 3.5, and 8.0 wt%)+water systems are measured by both a conventional isochoric (pVT) method and a stepwise differential scanning calorimeter (DSC) method. Both pVT and DSC methods demonstrate reliable and consistent hydrate phase equilibrium points of the HFC-134a hydrates in the presence of NaCl. The HFC-134a hydrate is identified as sII via powder X-ray diffraction. The dissociation enthalpies (ΔH_d) of the HFC-134a hydrates in the presence of NaCl are also measured with a high pressure micro-differential scanning calorimeter. The salinity results in significant thermodynamic inhibition of the HFC-134a hydrates, whereas it has little effect on the dissociation enthalpy of the HFC-134a hydrates. The experimental results obtained in this study can be utilized as foundational data for the hydrate-based desalination process.

Keywords: Gas Hydrate, Desalination, HFC-134a, Dissociation Enthalpy, Phase Behavior

INTRODUCTION

Gas hydrates are non-stoichiometric crystalline inclusion compounds that consist of water and guest molecules. The water molecules form hydrate frameworks with hydrogen-bonded cages, in which the guest molecules are incorporated. Gas hydrates exist in three different structures (structure I (sI), structure II (sII), and structure H (sH)), depending on the sizes and shapes of the cages. sI hydrates have two small 5^{12} cages and six large $5^{12}6^2$ cages with 46 water molecules in a unit cell, and they can capture small guest molecules such as methane, ethane, carbon dioxide, and hydrogen sulfide. sII hydrates are composed of 136 water molecules (16 small 5^{12} cages and 8 large $5^{12}6^4$ cages) and can generally trap larger guest molecules such as propane, isobutane, and cyclopentane. sH hydrates consist of 34 water molecules (three small 5^{12} cages, two medium $4^35^66^3$ cages, and one large $5^{12}6^8$ cage). In contrast to sI and sII hydrates, sH hydrates require additional gaseous guest molecules for the small 5^{12} and medium $4^35^66^3$ cages in order to stabilize the larger hydrocarbon guest molecules such as neohexane, methylcyclopentane, and methylcyclohexane in the large $5^{12}6^8$ cages [1,2].

Gas hydrates have been utilized in various fields: from exploitation of naturally occurring gas hydrates, natural gas storage and transportation, carbon dioxide capture and sequestration, to desalination [3-10]. Among their various applications, hydrate-based desalination has recently attracted significant attention because the need for desalination is increasing due to water shortages and the sources for desalination are not limited to seawater. For water containing high salinity from shale gas operations or CO_2 sequestration processes, the conventional desalination processes of distillation and reverse osmosis exhibit limited efficiencies due to the significant salinity in the produced water [11,12]. However, the hydrate-based desalination process is less influenced by the increased salinity in the water because it relies on a liquid-solid phase transition, which excludes salts and impurities from the cages during crystallization. In desalination via gas hydrate formation, appropriate hydrate-forming substances should be determined in order to operate the process in milder pressure and temperature conditions for economic competitiveness. Thermodynamic and kinetic studies have been conducted on possible guests such as SF_6, hydrofluorocarbons, CO_2, cyclopentane, and cyclohexane for hydrate-based desalination [5,8, 12-15].

Hydrofluorocarbons (HFCs), which are alternatives to chlorofluorocarbons (CFCs) and chlorohydrofluorocarbons (CHFCs) in air-conditioning systems, have also been known to form gas hydrates at relatively milder pressure and temperature conditions [16,17]. Although the phase equilibria of HFC hydrates including 1,1,1,2-tetrafluoroethane (HFC-134a), pentafluoroethane (HFC-125), and 1,1,1-trifluoroethane (HFC-143a) have already been examined, more attention should be given to the thermodynamic behavior, structural identification, and dissociation enthalpies of HFC hydrates in the presence of salts [13,16-18].

In this study, HFC-134a was selected as the hydrate former for

†To whom correspondence should be addressed.
E-mail: ywseo@unist.ac.kr
‡These authors contributed equally to this work and should be considered co-first authors.
ǂThis article is dedicated to Prof. Huen Lee on the occasion of his retirement from KAIST.

the hydrate-based desalination. To verify the influence of NaCl on the thermodynamic stability of the HFC-134a hydrate, the three-phase (hydrate (H) - liquid water (L_W) - vapor (V)) equilibria of the HFC-134a+NaCl (0, 3.5, and 8.0 wt%)+water systems were measured using both a conventional isochoric (pVT) method and a stepwise differential scanning calorimeter (DSC) method. The accurate structure of the HFC-134a hydrate was identified via powder X-ray diffraction (PXRD). For a better understanding of the thermal behavior and heat requirements for the hydrate-based desalination, the dissociation enthalpies (ΔH_d) of the HFC-134a hydrates in the presence of NaCl were also measured using a high pressure micro-differential scanning calorimeter (HP μ-DSC).

EXPERIMENTAL SECTION

1. Materials

Double-distilled and deionized water was used for all experiments. NaCl with a minimum purity of 99.5% was supplied by Sigma-Aldrich (USA). HFC-134a with a minimum purity of 99.9% was supplied by DuPont (USA).

2. Experimental Apparatus and Procedure

A high-pressure equilibrium vessel with an internal volume of 250 cm^3 was used to measure the three-phase (hydrate (H) - liquid water (L_w) - vapor (V)) equilibria of the HFC-134a+NaCl+water systems. The inner content was agitated vigorously with an impeller-type stirrer. The temperature of the inner content was measured by using a thermocouple, which was calibrated with an ASTM 63 C thermometer (H-B Instrument Company, USA) with a resolution of 0.1 K. A pressure transducer (S-10, WIKA, Germany) was used to measure the system pressure, and it was calibrated with a Heise Bourdon tube pressure gauge (Ashcroft Inc., USA) with an accuracy of ±0.1% for the full scale (0 to 10 MPa). For the equilibrium measurement, approximately 50 g of aqueous NaCl solution

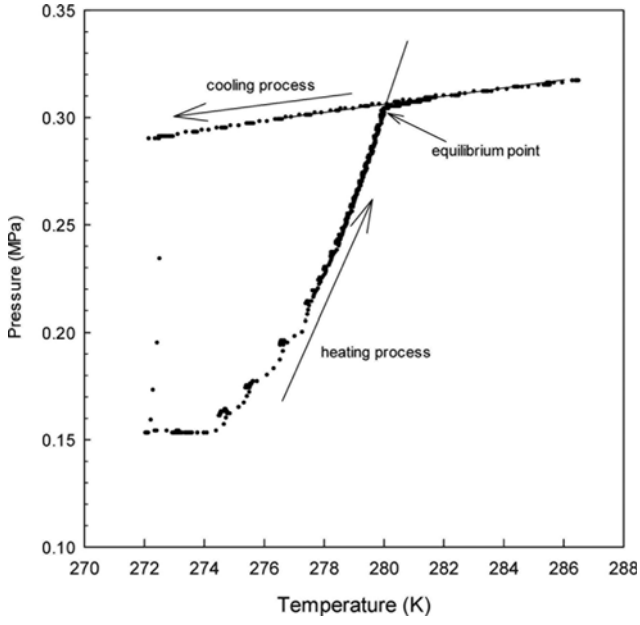

Fig. 1. Determination of the dissociation equilibrium point for the pure HFC-134a hydrate using an isochoric method.

(0, 3.5, and 8.0 wt%) was loaded into the equilibrium vessel; then, the vessel was submerged into a water bath whose temperature was controlled using an external circulator (RW-2025G, JEIO Tech., Republic of Korea). The residual air in the vessel and lines was removed by vacuum pump, and then the vessel was pressurized with HFC-134a gas to the desired pressure condition.

At first, an isochoric (pVT) method with step heating and cooling was used to measure the three-phase (H - L_w - V) equilibria. As depicted in Fig. 1, the temperature and pressure changes during the hydrate formation and dissociation were monitored. After a slight pressure decrease with a decrease in the temperature, an abrupt pressure drop occurred due to the gas hydrate formation. After sufficient time was given for the conversion of water to gas hydrate, the temperature was increased in steps of 0.1 K at time intervals of 180 min in order to accurately measure the equilibrium point in the presence of NaCl. The intersection between the thermal expansion line and the hydrate dissociation line was determined to be the three-phase (H - L_w - V) equilibrium point.

A high-pressure micro-differential scanning calorimeter (HP μ-DSC VII evo, Setaram Inc., France) was used to measure both dissociation enthalpies (ΔH_d) and phase equilibria of the HFC-134a hydrates in the presence of NaCl. The pressure monitoring system was set to have the same pressure transducer in the equilibrium vessel. The HP μ-DSC system consisted of reference and sample cells that were made from Hastelloy C276 to prevent corrosion and contamination, and the cells were surrounded by high sensitivity Peltier elements to ensure thermal contact with the calorimetric block. The maximum allowable work pressure for this system was 40 MPa, and the operable temperature range was from 228.15 K to 393.15 K with a resolution of 0.02 μW.

In the DSC experiments for the HFC-134a+NaCl+water systems, approximately 10 mg of NaCl solution (0, 3.5, and 8.0 wt%) was charged into the sample cell, and both reference and sample cells were flushed with HFC-134a gas after the residual air was removed by using a vacuum pump. After the HFC-134a gas was injected to the desired pressure, the sample solution was converted into HFC-134a hydrates by using the multi-cycle mode of cooling-heating. In this mode, the temperature of the HP μ-DSC cells was cooled to 243.15 K and heated to 274.15 K to generate metastable polyhedral water clusters, which caused the "memory effect" [19,20]. The multi-cycle mode of cooling-heating was terminated when the peaks from the ice formation or melting disappeared, as depicted in Fig. 2(a).

In this study, a stepwise DSC method was also used to measure the accurate H - L_W - V equilibria of the HFC-134a hydrates in the presence of NaCl. The temperature of the HP μ-DSC cells was increased with a step size of 0.1 K at time intervals of 60 min. As depicted in Fig. 2(b), at the beginning of the temperature rise, there was almost no heat flow change caused by the hydrate dissociation. However, after a while, sharp endothermic peaks appeared at every step of the temperature rise until the hydrate dissociation was completely terminated. After hydrate dissociation was completed, only the signals from the temperature rise were observed again. The point where the endothermic peaks that resulted from the hydrate dissociation disappeared and there were no more changes in the heat flow curves was determined to be the dissociation equilib-

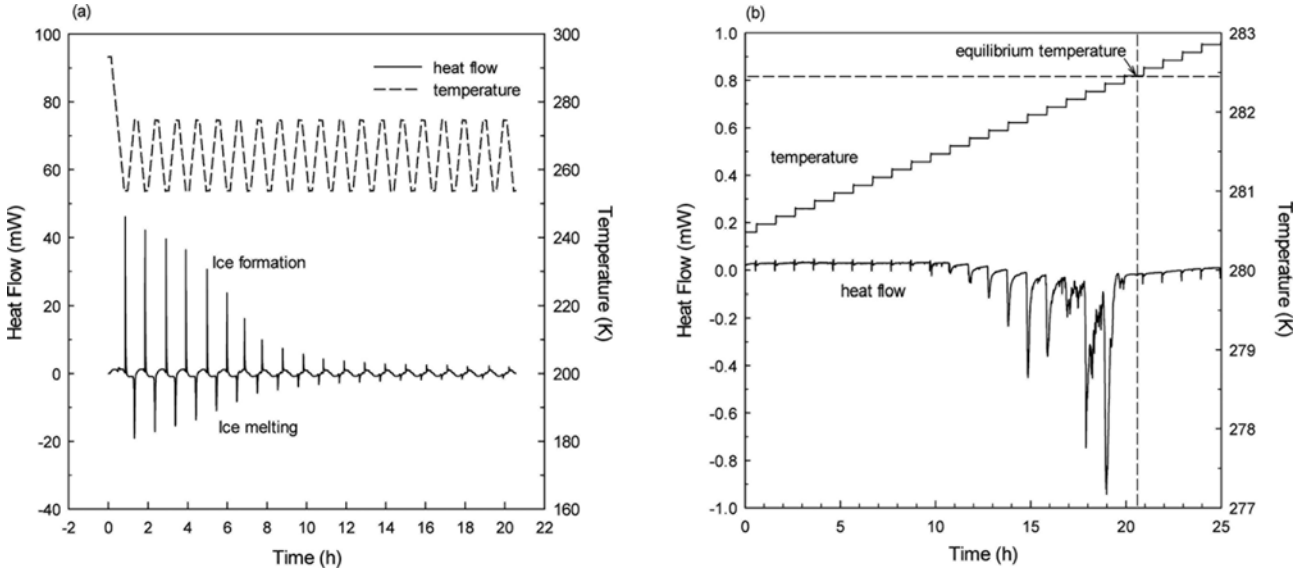

Fig. 2. Changes in the heat flow during (a) the multi-cycle mode of cooling-heating for the complete conversion of the solution to HFC-134a hydrate and (b) the hydrate dissociation using a stepwise mode.

rium temperature at the specified pressure.

To measure the ΔH_d of the HFC-134a hydrates in the presence of NaCl, the precise amount of water charged in the sample cell was calculated through comparing the experimentally measured enthalpy value of the ice melting for the charged solution and the known enthalpy of the ice melting from the literature [21,22]. Then, the HFC-134a gas was injected to the desired pressure, and the sample was completely converted into gas hydrate again through adopting the multi-cycle mode of cooling-heating. Then, the temperature of the HP μ-DSC cells was increased to 313.15 K at a heating rate of 0.5 K/min to dissociate the HFC-134a hydrates in the presence of NaCl. The final ΔH_d values were obtained from the integration of the endothermic peak in the final dissociation stage.

The crystalline structure of the HFC-134a hydrate was analyzed via powder X-ray diffraction (PXRD). The sample was prepared in the same apparatus used for the phase equilibrium measurements. After completion of the HFC-134a hydrate formation, the vessel was rapidly cooled with liquid nitrogen to prevent hydrate dissociation during the evacuation. The hydrate sample for the PXRD measurement was finely ground into particles with 50 μm diameters. The PXRD patterns of the HFC-134a hydrate were collected by using a Rigaku Geigerflex diffractometer with graphite-monochromatized Cu-Kα radiation (λ=1.5406 Å) with a step mode (fixed time of 3 s and step size of 0.02° for 2θ=5°-55° at 133.15 K). The Chekcell program was used for the refinement of the obtained PXRD patterns. A more detailed description of the experimental methods and procedures has been provided in previous papers [23-27].

RESULTS AND DISCUSSION

As presented in Fig. 3 and Table 1, the hydrate phase equilibria of the HFC-134a+NaCl (0, 3.5, and 8.0 wt%)+water systems were measured to examine the influence of NaCl on the thermodynamic stability of the HFC-134a hydrate. The stability conditions were determined by using the conventional isochoric (pVT) method as well as the stepwise differential scanning calorimeter (DSC) method. The H - L_W - V equilibrium points of the pure HFC-134a hydrate measured in this study were in good agreement with those by Liang et al. [16] and Hashimoto et al. [18]. The thermodynamic stability conditions of the HFC-134a hydrates in the presence of NaCl shifted to the inhibited regions represented by higher pressures at a given temperature or lower temperature at a given pressure depending on the NaCl concentrations.

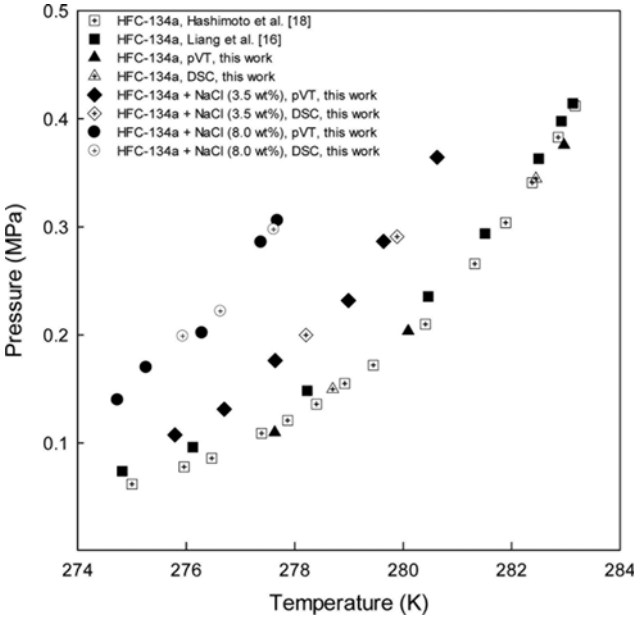

Fig. 3. Hydrate phase equilibria of the HFC-134a+NaCl (0, 3.5, and 8.0 wt%)+water systems (isochoric (pVT) method versus DSC method).

Table 1. HFC-134a hydrate phase equilibrium data in the presence of NaCl obtained from isochoric method and DSC method

NaCl concentration (wt%)	Isochoric method		DSC method	
	Temperature (K)	Pressure (MPa)	Temperature (K)	Pressure (MPa)
0	277.6	0.11	278.7	0.15
	280.1	0.20	282.5	0.34
	283.0	0.38		
3.5	275.8	0.11	279.9	0.29
	276.7	0.13	278.2	0.20
	277.6	0.18		
	279.0	0.23		
	279.6	0.29		
	280.6	0.36		
8.0	274.7	0.20	275.9	0.20
	275.3	0.17	276.6	0.22
	276.3	0.20	277.6	0.30
	277.4	0.29		
	277.7	0.31		

The conventional isochoric (pVT) method has been considered a reliable method that has been widely used to determine the hydrate phase equilibria [28-33]. However, for salt-containing solutions, this isochoric method can be a very time-consuming process to determine the accurate hydrate phase equilibrium points, because the inhomogeneous distribution of the salinity in the system causes irregular hydrate dissociation and, therefore, a significantly longer time is required to reach an equilibrium state at each temperature ramping step. Several investigations have been conducted on less time-consuming, but accurate, techniques for determination of the hydrate phase equilibria in the presence of salts [34-36]. The DSC method has recently been introduced as a reliable and less time-consuming technique for hydrate equilibrium measurements [22,25,37]. In the DSC method, the dissociation equilibrium temperature is generally determined from the onset temperature (T_{onset}), which is defined as the intersection of an extrapolated baseline with a line tangent to the inflection of the endothermic heat flow curve [26,38]. However, the salinity of the solution inevitably increases as the hydrate formation proceeds and extremely high salt-containing solutions remain at the end of the hydrate formation, because the hydrate cages exclude salt ions during crystallization. Likewise, these extremely high salt-containing solutions become diluted as the hydrate dissociation proceeds. This continuous and gradual change in salinity during the dissociation process results in a broader endothermic peak, which makes it difficult to determine the accurate T_{onset} of the HFC-134a hydrates in the presence of NaCl. In addition, the heat flow curve during the hydrate dissociation can fluctuate due to the localized inhomogeneity caused by the limitation of the mass transfer [39,40]. To overcome the influence of the salinity change on the T_{onset}, the stepwise method can be used for salt-containing systems. Unlike the continuous temperature ramping method that can provide T_{onset}, the stepwise method can provide a final dissociation equilibrium temperature without the influence of the salinity change because the equilibrium temperature is determined at the point where the heat flow curve returns to the baseline and the hydrate dissociation is completely terminated.

As presented in Fig. 3 and Table 1, both the conventional isochoric method and stepwise DSC method demonstrated consistent stability conditions for the HFC-134a hydrates. In the presence of NaCl, a stronger inhibition effect was observed for the 8.0 wt% NaCl solution compared with the 3.5 wt% NaCl solution. In the NaCl solutions, Na^+ and Cl^- were not enclathrated into the cages of the gas hydrates, but they disrupted the hydrogen bonding of the water molecules in the host lattices of the HFC-134a hydrates, thereby weakening the thermodynamic stability and causing thermodynamic inhibition. The hydrate phase behavior of the HFC-

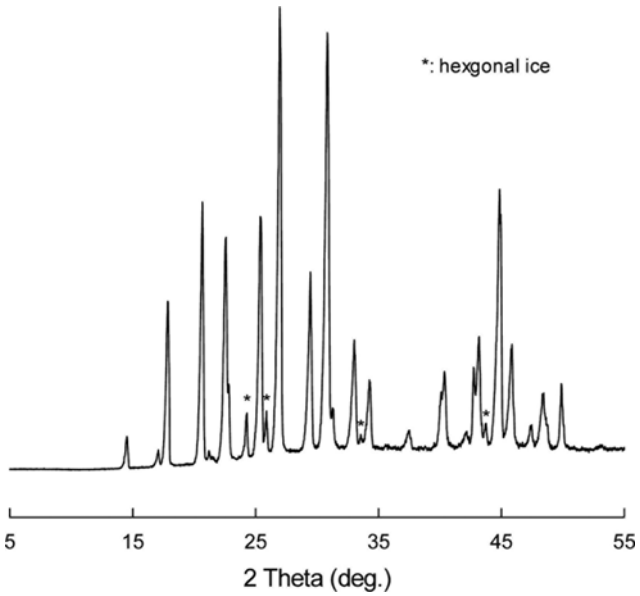

Fig. 4. Powder X-ray diffraction patterns of the pure HFC-134a hydrate.

134a hydrates in the presence of NaCl can provide foundational information to predict and estimate the operating conditions for the HFC-134a hydrate-based desalination.

Considering that the hydrate structure is closely related to the operable capacity of the hydrate-based desalination process, the precise crystalline structure of the HFC-134a hydrate is a significant prerequisite for this application. In this study, the crystalline structure of the HFC-134a hydrate was identified using PXRD. The PXRD patterns of the pure HFC-134a hydrate in Fig. 4 indicate the sII hydrate formation, and these were indexed by using a regular cubic cell with a space group of *Fd3m*. The lattice parameter of the sII HFC-134a hydrate was a=17.18 Å. Using microscopic analyses such as PXRD and NMR, several researchers have reported that the presence of salts did not affect the crystalline structure of the gas hydrates because salts do not participate in building the hydrate cages [15,41]. Therefore, it is expected that the HFC-134a+NaCl+water systems will also form sII hydrates regardless of the NaCl concentrations.

The dissociation enthalpy (ΔH_d) of the HFC-134a hydrate is also an essential factor in designing and optimizing the hydrate-based desalination process, considering that it is directly related to the heat liberated or absorbed during the hydrate formation and dissociation. Despite the importance of accurate ΔH_d values of the HFC-134a hydrates, they have not yet been experimentally measured. In this study, the ΔH_d values of the HFC-134a+NaCl (0, 3.5, and 8.0 wt%)+water systems were measured with an HP μ-DSC. Fig. 5 presents the dissociation thermograms of the HFC-134a hydrates at different salinities. The HFC-134a hydrates in the presence of NaCl exhibited broad endothermic peaks, whereas the pure HFC-134a hydrate exhibited a relatively sharp endothermic peak. The endothermic peaks became significantly broader as the NaCl concentration increased. During the dissociation process of the HFC-134a hydrate with a higher NaCl concentration in the HP μ-DSC, the gas hydrate began to dissociate at a lower temperature and, as the gas hydrate dissociated, the equilibrium temperature of the system continued to increase because the local NaCl concentration in the aqueous phase continued to decrease with the hydrate dissociation.

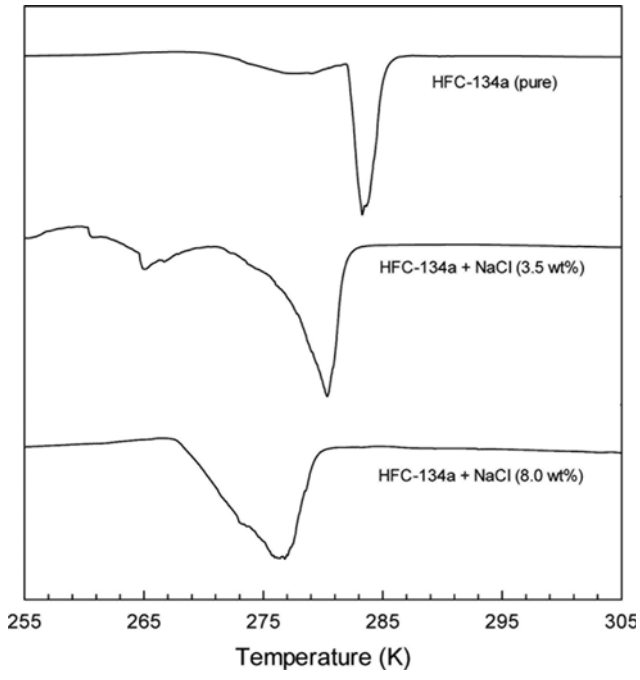

Fig. 5. Dissociation thermograms of the HFC-134a hydrates at different salinities.

Considering the molecular size of HFC-134a, it is reasonably assumed that the HFC-134a molecules occupy only the large $5^{12}6^4$ cage of sII hydrates; therefore, the hydration number of the HFC-134a hydrate is 17. As seen in Table 2, the ΔH_d value of the pure HFC-134a hydrate was 146.0±0.5 kJ/mole gas, which is in good agreement with the literature value that was calculated from the slope of the phase equilibrium curve (dp/dT) by using the Clapeyron equation [18]. The ΔH_d values of the HFC-134a hydrates in the presence of NaCl were measured to be 145.7±0.2 and 145.1±2.1 kJ/mole gas for the 3.5 and 8.0 wt% solutions, respectively. It was confirmed from the experimentally measured ΔH_d values that the salinity had little effect on the dissociation enthalpy of the HFC-134a hydrates. The slightly lower ΔH_d value with a slightly larger deviation for the HFC-134a+NaCl (8.0 wt%) hydrate can be attributed to the slightly higher uncertainty involved in integrating the broader endothermic peak.

CONCLUSIONS

Three-phase (H-L_W-V) equilibria of HFC-134a hydrates in the presence of NaCl were measured through both a conventional isochoric (pVT) method and a stepwise DSC method. Both methods provided reliable and consistent hydrate phase equilibrium data of the HFC-134a hydrates in the presence of NaCl. HFC-134a hydrate was revealed to be sII via PXRD. A HP μ-DSC was also used to determine the accurate dissociation enthalpies of the HFC-134a hydrates in the presence of NaCl. The presence of NaCl demonstrated a thermodynamic inhibition effect on the H-L_W-V equilibria depending on NaCl concentrations, but had little effect on dissociation enthalpies of HFC-134a hydrates. The experimental results covering phase behavior, structure identification, and dissociation enthalpies of HFC-134a hydrates can provide fundamental information and better understanding of the hydrate-based

Table 2. Dissociation enthalpies of HFC-134a hydrates in NaCl solutions

System	ΔH (J/g-water)	ΔH (J/g-hydrate)	ΔH (kJ/mole gas)	Hydration number
HFC-134a	476.9±1.5	357.6±1.1	146.0±0.5	17.0
HFC-134a+NaCl (3.5 wt%)	476.2±0.6	357.2±0.4	145.7±0.2	17.0
HFC-134a+NaCl (8.0 wt%)	474.1±7.1	355.5±5.3	145.1±2.1	17.0

desalination process.

ACKNOWLEDGEMENTS

This research was supported by Mid-career Research Program through the National Research Foundation of Korea (NRF) founded by the Ministry of Science, ICT & Future Planning (NRF-2014R1A2A1A11049950) and also by the National Research Foundation of Korea (NRF) Grant funded by the Korean Government (MSIP) (No. NRF-2015R1A5A7037825).

REFERENCES

1. E. D. Sloan and C. A. Koh, *Clathrate Hydrates of Natural Gases*, CRC Press/Taylor & Francis, Boca Raton, FL (2008).
2. C. Giavarini and K. Hester, *Gas Hydrates: Immense Energy Potential and Environmental Challenges*, Springer, London (2011).
3. P. Linga, A. Adeyemo and P. Englezos, *Environ. Sci. Technol.*, **42**, 315 (2007).
4. S. Watanabe, S. Takahashi, H. Mizubayashi, S. Murata and H. Murakami, *Proceedings of the 6th International Conference on Gas Hydrates*, 6 (2008).
5. D. Corak, T. Barth, S. Høiland, T. Skodvin, R. Larsen and T. Skjetne, *Desalination*, **278**, 268 (2011).
6. X.-S. Li, C.-G. Xu, Z.-Y. Chen and H.-J. Wu, *Energy*, **36**, 1394 (2011).
7. S. Park, S. Lee, Y. Lee and Y. Seo, *Environ. Sci. Technol.*, **47**, 7571 (2013).
8. S. Han, J.-Y. Shin, Y.-W. Rhee and S.-P. Kang, *Desalination*, **354**, 17 (2014).
9. Y. Lee, Y. Kim and Y. Seo, *Environ. Sci. Technol.*, **49**, 8899 (2015).
10. S. Kim, S.-P. Kang and Y. Seo, *Chem. Eng. J.*, **276**, 205 (2015).
11. H. Lee, H. Ryu, J.-H. Lim, J.-O. Kim, J. D. Lee and S. Kim, *Desalin. Water Treat.* (2015), DOI:10.1080/19443994.2015.1049405.
12. J.-H. Cha and Y. Seol, *ACS Sustainable Chem. Eng.*, **1**, 1218 (2013).
13. Y. Seo, H. Tajima, A. Yamasaki, S. Takeya, T. Ebinuma and F. Kiyono, *Environ. Sci. Technol.*, **38**, 4635 (2004).
14. I. Cha, S. Lee, J. D. Lee, G.-w. Lee and Y. Seo, *Environ. Sci. Technol.*, **44**, 6117 (2010).
15. Y. Seo, D. Moon, C. Lee, J.-W. Park, B.-S. Kim, G.-W. Lee, P. Dotel, J.-W. Lee, M. Cha and J.-H. Yoon, *Environ. Sci. Technol.*, **49**, 6045 (2015).
16. D. Liang, K. Guo, R. Wang and S. Fan, *Fluid Phase Equilib.*, **187**, 61 (2001).
17. T. Akiya, T. Shimazaki, M. Oowa, M. Matsuo and Y. Yoshida, *Int. J. Therm.*, **20**, 1753 (1999).
18. S. Hashimoto, T. Makino, Y. Inoue and K. Ohgaki, *J. Chem. Eng. Data*, **55**, 4951 (2010).
19. S. Takeya, A. Hori, T. Hondoh and T. Uchida, *J. Phys. Chem. B.*, **104**, 4164 (2000).
20. P. Buchanan, A. K. Soper, H. Thompson, R. E. Westacott, J. L. Creek, G. Hobson and C. A. Koh, *J. Chem. Phys.*, **123**, 164507 (2005).
21. G. Hakvoort, *J. Therm. Anal. Calorim.*, **41**, 1551 (1994).
22. A. Gupta, J. Lachance, E. D. Sloan Jr. and C. A. Koh, *Chem. Eng. Sci.*, **63**, 5848 (2008).
23. Y. Seo and H. Lee, *J. Phys. Chem. B.*, **106**, 9668 (2002).
24. S. Lee, Y. Lee, S. Park, Y. Kim, J. D. Lee and Y. Seo, *J. Phys. Chem. B.*, **116**, 9075 (2012).
25. S. Lee, Y. Lee, J. Lee, H. Lee and Y. Seo, *Environ. Sci. Technol.*, **47**, 13184 (2013).
26. Y. Lee, S. Lee, J. Lee and Y. Seo, *Chem. Eng. J.*, **246**, 20 (2014).
27. Y. Lee, Y. Kim, J. Lee, H. Lee and Y. Seo, *Appl. Energy*, **150**, 120 (2015).
28. T. Sugahara, S. Murayama, S. Hashimoto and K. Ohgaki, *Fluid Phase Equilib.*, **233**, 190 (2005).
29. A. H. Mohammadi, R. Anderson and B. Tohidi, *AIChE J.*, **51**, 2825 (2005).
30. T. Uchida, R. Ohmura, I. Y. Ikeda, J. Nagao, S. Takeya and A. Hori, *J. Phys. Chem. B.*, **110**, 4583 (2006).
31. S.-P. Kang, J.-W. Lee and H.-J. Ryu, *Fluid Phase Equilib.*, **274**, 68 (2008).
32. Y. Seo, S.-P. Kang, S. Lee and H. Lee, *J. Chem. Eng. Data*, **53**, 2833 (2008).
33. S. Lee, Y. Lee, S. Park and Y. Seo, *J. Chem. Eng. Data*, **55**, 5883 (2010).
34. B. Tohidi, R. Burgass, A. Danesh, K. Østergaard and A. Todd, *Ann. N.Y. Acad. Sci.*, **912**, 924 (2000).
35. M. Mohammad-Taheri, A. Z. Moghaddam, K. Nazari and N. G. Zanjani, *Fluid Phase Equilib.*, **338**, 257 (2013).
36. M. Cha, Y. Hu and A. K. Sum, *Fluid Phase Equilib.*, In Press (2015).
37. D. Dalmazzone, M. Kharrat, V. Lachet, B. Fouconnier and D. Clausse, *J. Therm. Anal. Calorim.*, **70**, 493 (2002).
38. S. Lee, S. Park, Y. Lee, J. Lee, H. Lee and Y. Seo, *Langmuir.*, **27**, 10597 (2011).
39. P. G. Lafond, K. A. Olcott, E. D. Sloan, C. A. Koh and A. K. Sum, *J. Chem. Thermodyn.*, **48**, 1 (2012).
40. W. Lin, D. Dalmazzone, W. Fürst, A. Delahaye, L. Fournaison and P. Clain, *J. Chem. Thermodyn.*, **61**, 132 (2013).
41. S. Lee and Y. Seo, *Energy Fuels*, **24**, 6074 (2010).